

Power laws and collapsing dynamics of a trapped Bose-Einstein condensate with attractive interactions

Hiroki Saito and Masahito Ueda

*Department of Physics, Tokyo Institute of Technology, Tokyo 152-8551, Japan
and CREST, Japan Science and Technology Corporation (JST), Saitama 332-0012, Japan*

(October 27, 2018)

The critical behavior of collective modes and the collapsing dynamics of trapped Bose-Einstein condensates with attractive interactions are studied analytically and numerically. The time scales of these dynamics both below and above the critical point of the collapse are found to obey power laws with a single parameter of $N/N_c - 1$, where N is the number of condensate atoms and N_c is the critical number. The collapsing condensate eventually undergoes rapid implosion, which occurs several times intermittently, and then the implosion turns to an explosion. The release energy of the explosion is found to be proportional to the square of the interaction strength, inversely proportional to the three-body recombination rate, and independent of the number of condensate atoms and the trap frequency.

03.75.Fi, 05.30.Jp, 32.80.Pj, 82.20.Mj

I. INTRODUCTION

Bose-Einstein condensates (BECs) of trapped atomic vapor have been realized in several species. The static and dynamical properties of BEC crucially depend on the sign of the interatomic interaction, which is, without an external field, repulsive for ^{87}Rb [1], ^{23}Na [2], and ^1H [3], and attractive for ^7Li [4] and ^{85}Rb [5]. The interactions can be manipulated by applying the electric or magnetic field, as the scattering length is sensitive to the external field near the Feshbach resonance [6]. Using this technique, one can control not only the strength of the interaction [7] but also its sign [5].

In a spatially uniform three-dimensional system, the attractive interaction between atoms makes BEC unstable. In a spatially confined system, however, the zero-point energy serves as a kinetic obstacle against collapse, allowing metastable BEC to be formed if the number N of BEC atoms is below a certain critical value N_c [8–17]. Various properties of BEC below and above N_c have been predicted. Just below N_c , BEC may collapse via macroscopic quantum tunneling [18,19,14,15,20]. When N exceeds N_c , BEC becomes unstable and exhibits complicated collapsing dynamics. Kagan *et al.* [21] have predicted that the implosion of BEC eventually turns to explosion due to loss of atoms by three-body molecular recombination. Because the lost atoms are replenished by a thermal cloud, the number of BEC atoms again exceeds N_c , leading to the collapse-and-growth cy-

cles of BEC [22,23,21]. Such dynamic behavior of collapsing BEC has been explored with recent Rice experiments [24]. Ueda and Huang [25] have shown that the collapse occurs locally within a small region around the center of the trap, and this result has been verified numerically [26]. We have predicted [27] that implosions occur intermittently and in rapid sequence due to competition between a loss of atoms and the attractive interactions. When the interaction is suddenly switched from repulsive to attractive by using the Feshbach resonance, various patterns such as a shell structure may be formed in the atomic density [27].

In recent experiments with ^{85}Rb at JILA [5], nearly pure condensates have been produced in which the number of atoms can be fixed, and both the strength and sign of the interaction can be controlled by using the Feshbach resonance. These results suggest that N_c can be tuned with the number of BEC atoms held fixed. We may thus study the critical behavior of BEC by controlling the relevant parameters.

In the present paper, we study the dynamics of BEC with attractive interactions at zero temperature both below and above the critical point. We find that both collective-mode frequencies just below the critical point and the time it takes BEC just above this critical point to collapse obey power laws with a single parameter $N/N_c - 1$. We use a time-dependent Gaussian trial wave function to analytically study collective-mode frequencies and the collapsing dynamics, and compare the obtained results with those obtained by numerically solving the Bogoliubov equations and the time-dependent Gross-Pitaevskii (GP) equation [28]. When the atomic loss due to inelastic collisions is taken into account, the collapsing condensate undergoes intermittent implosions followed by an explosion. We find the energy released by the explosion is proportional to g^2/L_3 and independent of the number of atoms and the trap frequency, where g is the strength of the interaction and L_3 is a coefficient of the three-body recombination rate.

This paper is organized as follows. Section II formulates the problem and introduces an effective-potential model based on a time-dependent Gaussian variational wave function. Section III discusses the collective oscillations of BEC below N_c . Section IV analyzes the collapsing dynamics of BEC above N_c . In both regimes, our analytical and numerically exact results are in excellent agreement. Section V discusses the dynamics of implo-

sion and explosion of BEC by incorporating the atomic loss into our theory. Finally, section VI summarizes our results.

II. FORMULATION OF THE PROBLEM

We consider a system of Bose-condensed atoms with mass m and s-wave scattering length a , confined in an isotropic parabolic potential. The Hamiltonian for the system is given by

$$\hat{H} = \int d\mathbf{r} \hat{\psi}^\dagger(\mathbf{r}) \left[-\frac{\hbar^2}{2m} \nabla^2 + \frac{m\omega_0^2 \mathbf{r}^2}{2} + \frac{2\pi\hbar^2 a}{m} \hat{\psi}^\dagger(\mathbf{r}) \hat{\psi}(\mathbf{r}) \right] \hat{\psi}(\mathbf{r}), \quad (1)$$

where $\hat{\psi}(\mathbf{r})$ is the field operator of the atoms. The transition amplitude of the system from an initial ψ_i to a final state ψ_f is expressed in terms of path integrals as

$$\langle \psi_f | e^{-\frac{i}{\hbar} \hat{H}(t_f - t_i)} | \psi_i \rangle = \int \mathcal{D}\psi \mathcal{D}\psi^* e^{\frac{i}{\hbar} S[\psi, \psi^*]}, \quad (2)$$

where the action $S[\psi, \psi^*]$ is given by

$$S[\psi, \psi^*] = N\hbar \int d\mathbf{r} \int dt \left[i\psi^* \frac{\partial}{\partial t} \psi + \frac{1}{2} \psi^* \nabla^2 \psi - \frac{r^2}{2} \psi^* \psi - \frac{g}{2} (\psi^* \psi)^2 \right]. \quad (3)$$

Here the length, time, and ψ are normalized in units of $d_0 = (\hbar/m\omega_0)^{1/2}$, ω_0^{-1} and $(N/d_0^3)^{1/2}$, respectively, and $g \equiv 4\pi Na/d_0$. The wave function is then normalized to unity. Separating $\psi(\mathbf{r}, t)$ into amplitude and phase as $\psi(\mathbf{r}, t) = A(\mathbf{r}, t)e^{i\phi(\mathbf{r}, t)}$, and substituting this into Eq. (3), we obtain

$$S = N\hbar \int d\mathbf{r} \int dt \left[i\dot{A}A - A^2\dot{\phi} + \frac{1}{2}A\nabla^2 A - \frac{1}{2}A^2(\nabla\phi)^2 + \frac{i}{2}\nabla(A^2\nabla\phi) - \frac{r^2}{2}A^2 - \frac{g}{2}A^4 \right]. \quad (4)$$

The requirement that the action be stationary with respect to small variations in ϕ leads to

$$\frac{\partial A^2}{\partial t} + \nabla(A^2\nabla\phi) = 0. \quad (5)$$

This is nothing but the equation of continuity that guarantees the conservation of the number of atoms. The stationary condition for small variations in A is, together with Eq. (5), equivalent to the GP equation

$$i\frac{\partial}{\partial t}\psi = -\frac{1}{2}\nabla^2\psi + \frac{r^2}{2}\psi + g|\psi|^2\psi. \quad (6)$$

For the case of attractive interactions, it is reasonable to assume that the amplitude takes a Gaussian form,

with its width reduced due to the attractive interaction. The validity of this Gaussian approximation will be examined by comparison with the numerically exact results in Secs. III and IV. Because we want to study the dynamics of BEC, we allow the amplitude $A(\mathbf{r}, t)$ to vary in time as [9,14]

$$A(\mathbf{r}, t) = \sqrt{\frac{1}{\pi^{3/2}d_x(t)d_y(t)d_z(t)}} \times \exp \left[-\frac{x^2}{2d_x^2(t)} - \frac{y^2}{2d_y^2(t)} - \frac{z^2}{2d_z^2(t)} \right], \quad (7)$$

where $d_i(t)$ ($i = x, y, z$) is a time-dependent real variational parameter characterizing the width of the wave function along the i -axis. It can be shown that the equation of continuity (5) and the requirement that there should be no mass current both at the origin and at infinity uniquely determines the phase as

$$\phi(\mathbf{r}, t) = \frac{\dot{d}_x(t)}{2d_x(t)}x^2 + \frac{\dot{d}_y(t)}{2d_y(t)}y^2 + \frac{\dot{d}_z(t)}{2d_z(t)}z^2. \quad (8)$$

We thus obtain the variational wave function as [29]

$$\psi_{\text{var}}(\mathbf{r}, t) = \sqrt{\frac{1}{\pi^{3/2}d_x(t)d_y(t)d_z(t)}} \exp \left\{ -\frac{x^2}{2d_x^2(t)}[1 - i\dot{d}_x(t)d_x(t)] - \frac{y^2}{2d_y^2(t)}[1 - i\dot{d}_y(t)d_y(t)] - \frac{z^2}{2d_z^2(t)}[1 - i\dot{d}_z(t)d_z(t)] \right\}. \quad (9)$$

The imaginary terms in the exponent in Eq. (9) describe the mass current associated with the change in the width of the wave function. To find the most probable Feynman path within a functional space of the complex Gaussian wave function (9), we substitute Eq. (9) into Eq. (3), obtaining

$$S = \frac{N\hbar}{4} \int dt \left[\sum_{i=x,y,z} \left(\dot{d}_i^2(t) - \frac{1}{d_i^2(t)} - d_i^2(t) + \dot{d}_i(t) \right) - \frac{\gamma}{d_x(t)d_y(t)d_z(t)} \right], \quad (10)$$

where $\gamma \equiv \frac{4N}{\sqrt{2\pi}} \frac{a}{d_0}$. The stationary condition $\delta S/\delta d_i = 0$ gives an equation of motion for $d_i(t)$ as [29]

$$\ddot{d}_i(t) = -d_i(t) + d_i^{-3}(t) + \frac{\gamma}{2d_x(t)d_y(t)d_z(t)d_i(t)} = -\frac{\partial V_{\text{eff}}}{\partial d_i}, \quad (11)$$

where

$$V_{\text{eff}} \equiv \frac{1}{2} \sum_{i=x,y,z} (d_i^2 + d_i^{-2}) + \frac{\gamma}{2d_x d_y d_z} \quad (12)$$

may be viewed as an effective potential for the widths of the wave function $d_i(t)$ [14,29].

III. POWER-LAW BEHAVIOR OF COLLECTIVE MODES

It has been predicted in Ref. [15] that as the criticality is reached, the monopole mode becomes softer according to the one-fourth power $1 - N/N_c$. In Ref. [15], however, a sum rule is invoked in order to determine the numerical coefficient. Here we develop a general theory that determines both the power and the numerical coefficient.

For an isotropic trapping potential, the stationary point of Eq. (11), $d_x = d_y = d_z \equiv d_{\text{st}}$, is determined by a positive root of

$$d_{\text{st}}^5 - d_{\text{st}} - \frac{\gamma}{2} = 0. \quad (13)$$

For the case of attractive interaction $\gamma < 0$, this equation has a positive root if the strength of the interaction $|\gamma|$ is smaller than the critical value γ_c [9,10],

$$|\gamma| < \gamma_c \equiv \frac{8}{5^{5/4}}, \quad (14)$$

where $|\gamma| = \gamma_c$ corresponds to $d_{\text{st}} = r_c \equiv 5^{-1/4}$. The stationary point d_{st} is always greater than r_c for $|\gamma| < \gamma_c$. The stability condition is given by

$$\det \left(\frac{\partial^2 V_{\text{eff}}}{\partial d_i \partial d_j} \right) \bigg|_{d=d_{\text{st}}} = (d_{\text{st}}^{-4} - 5)(2d_{\text{st}}^{-4} + 2)^2 < 0, \quad (15)$$

where the derivative is evaluated at the stationary point $d_x = d_y = d_z = d_{\text{st}}$. It follows from Eqs. (15) and (13) that the necessary and sufficient condition for BEC to have a metastable state is $|\gamma| < \gamma_c$.

Let $u_i(t) \equiv d_i(t) - d_{\text{st}}$ be the deviations of $d_i(t)$ from its stationary point at time t . Small oscillations of these quantities are governed by

$$\ddot{u}_i(t) = - \sum_{j=x,y,z} \frac{\partial^2 V_{\text{eff}}}{\partial d_i \partial d_j} \bigg|_{d=d_{\text{st}}} u_j(t). \quad (16)$$

Substituting $u_i(t) = u_i(0)e^{-i\omega t}$ into this yields an eigenvalue matrix equation:

$$\begin{bmatrix} \omega^2 - d_{\text{st}}^{-4} - 3 & d_{\text{st}}^{-4} - 1 & d_{\text{st}}^{-4} - 1 \\ d_{\text{st}}^{-4} - 1 & \omega^2 - d_{\text{st}}^{-4} - 3 & d_{\text{st}}^{-4} - 1 \\ d_{\text{st}}^{-4} - 1 & d_{\text{st}}^{-4} - 1 & \omega^2 - d_{\text{st}}^{-4} - 3 \end{bmatrix} \begin{bmatrix} u_x \\ u_y \\ u_z \end{bmatrix} = 0. \quad (17)$$

For this equation to have nontrivial solutions, we should have

$$\det \left(\omega^2 \delta_{ij} - \frac{\partial^2 V_{\text{eff}}}{\partial d_i \partial d_j} \right) \bigg|_{d=d_{\text{st}}} = (\omega^2 + d_{\text{st}}^{-4} - 5)(\omega^2 - 2d_{\text{st}}^{-4} - 2)^2 = 0. \quad (18)$$

Hence, we have the frequency of the monopole mode ω_M and that of the doubly degenerate quadrupole mode ω_Q as [30,29]

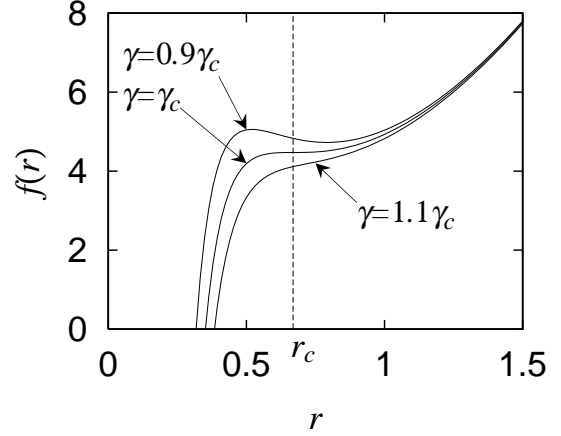


FIG. 1. The effective potential $f(r) = 3r^2 + 3r^{-2} + \gamma r^{-3}$ for the width r of BEC with attractive interactions for $|\gamma| = \gamma_c = 8 \cdot 5^{-5/4}$, $|\gamma| = 0.9\gamma_c$, and $|\gamma| = 1.1\gamma_c$. The dashed line shows the inflection point r_c at $|\gamma| = \gamma_c$.

$$\omega_M = \sqrt{5 - d_{\text{st}}^{-4}}, \quad (19)$$

$$\omega_Q = \sqrt{2(1 + d_{\text{st}}^{-4})}. \quad (20)$$

The eigenvector corresponding to the monopole mode is given by $(u_x, u_y, u_z) = (1, 1, 1)$, and therefore $d_x(t) = d_y(t) = d_z(t) \equiv r(t)$ always hold. Substituting this into Eq. (10) yields an effective action for the monopole mode,

$$S_M = \frac{N\hbar}{4} \int dt [3\dot{r}^2 - f(r) + 3\dot{r}], \quad (21)$$

where

$$f(r) = 3r^{-2} + 3r^2 + \gamma r^{-3} \quad (22)$$

may be viewed as an effective potential for $r(t)$.

The forms of the function $f(r)$ in the vicinity of $|\gamma| = \gamma_c$ are illustrated in Fig. 1 [29,22]. The potential $f(r)$ is a monotonically increasing function when $|\gamma| > \gamma_c$ and has a local minimum when $|\gamma| < \gamma_c$, indicating that γ_c is the critical strength of the interaction above which the condensate collapses upon itself. In other words, when the number of atoms exceeds the critical value

$$N_c \equiv \frac{2\sqrt{2\pi}d_{\text{st}}}{5^{5/4}|a|}, \quad (23)$$

the parameter $r(t)$ slides down the potential in time to $r(t) \rightarrow 0$, and the central density of the wave function grows unlimitedly. In contrast, when the number of atoms is smaller than N_c , $f(r)$ has a local minimum at which a metastable BEC is formed.

For $|\gamma|$ slightly below γ_c , we set $|\gamma| = \gamma_c - \delta\gamma$ and $d_{\text{st}} = r_c + \delta d$, and expand Eqs. (13), (19), and (20) in small quantities $\delta\gamma$ and δd . We then obtain

$$\frac{\delta d}{r_c} = \sqrt{\frac{2}{5} \left(1 - \frac{N}{N_c}\right)}, \quad (24)$$

$$\omega_M = \sqrt{20 \frac{\delta d}{r_c}}, \quad (25)$$

$$\omega_Q = \sqrt{12 - 40 \frac{\delta d}{r_c}}. \quad (26)$$

Substituting Eq. (24) into Eqs. (25) and (26), we obtain

$$\omega_M = 160^{1/4} \left(1 - \frac{N}{N_c}\right)^{1/4}, \quad (27)$$

$$\omega_Q = \sqrt{12 - 8 \sqrt{10 \left(1 - \frac{N}{N_c}\right)}}. \quad (28)$$

The result (27) agrees with that of Ref. [15] up to the numerical coefficient.

Figure 2 compares the analytic results (19) and (20) (solid curves) with those (dashed curves) obtained by numerically diagonalizing the Bogoliubov equations [31]. Since the Gaussian approximation overestimates the critical number of atoms N_c , the numerically exact value of N_c is used for the dashed curves in Fig. 2. In Fig. 2 (a), $\sqrt{5}$ and $\sqrt{2}$ indicate the Thomas-Fermi limits for the monopole and quadrupole modes, respectively [30]. The numerical and analytic results are in excellent agreement for an extensive range of $1 - N/N_c$, and the power law of ω_M for $1 - N/N_c \ll 1$ described in Eq. (27) is clearly illustrated in Fig. 2 (b).

IV. COLLAPSING DYNAMICS OF BEC

We assume that BEC is initially prepared in a metastable state with γ slightly smaller than γ_c . We then suddenly tighten the trap potential or increase $|a|$ by a technique such as the Feshbach resonance [7,5], so that $|\gamma| = \gamma_c + \delta\gamma$ slightly exceeds γ_c . BEC then begins to collapse. Although the collapsing behavior and its time scale are numerically studied in Refs. [29,23,26], no analytic forms have been reported for them.

The effective Lagrangian for the monopole mode is obtained from Eq. (21) as

$$L_M = \frac{N\hbar}{4} (3\dot{r}^2 - 3r^{-2} - 3r^2 + |\gamma|r^{-3}), \quad (29)$$

and the equation of motion reads

$$\ddot{r}(t) = r^{-3}(t) - r(t) - \frac{|\gamma|}{2} r^{-4}(t). \quad (30)$$

Integrating Eq. (30) with initial conditions $r(0) = r_c$ and $\dot{r}(0) = 0$ gives

$$\frac{dr}{dt} = -\sqrt{\frac{1}{3} [f(r_c) - f(r)]}. \quad (31)$$

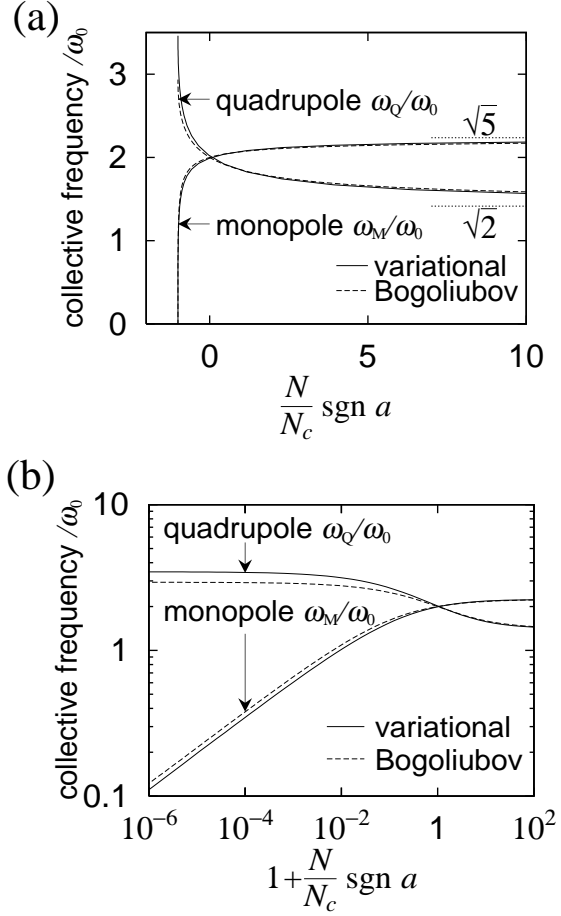


FIG. 2. The frequencies of the monopole and quadrupole modes ω_M and ω_Q , normalized by the trap frequency ω_0 as a function of $N/N_c \text{sgn } a$, where $\text{sgn } a = 1, 0$ and -1 for $a > 0$, $a = 0$, and $a < 0$, respectively. The solid curves show the results of the variational method, and the dashed curves show the results obtained by numerically diagonalizing the Bogoliubov equations. The dotted lines at $\sqrt{5}$ and $\sqrt{2}$ show the Thomas-Fermi limits of the monopole and quadrupole modes, respectively. The curves in (b) show the same data as in (a) on a logarithmic scale to clarify the power-law behavior of the monopole mode.

Taking $r(t) = r_c - x(t)$ and expanding the right-hand side of Eq. (31) up to the third power of $x(t)$, we obtain

$$\left(\frac{dx(t)}{dt}\right)^2 = 5\delta\gamma x(t) + 2 \cdot 5^{5/4} \delta\gamma x^2(t) + \frac{4 \cdot 5^{5/4}}{3} x^3(t). \quad (32)$$

The initial stage of the collapse, where $x(t) \ll 1$, is dominated by the first two terms on the right-hand side of Eq. (32). Integrating Eq. (32) by keeping only these two terms, we obtain

$$x(t) \simeq \frac{1}{4 \cdot 5^{1/4}} \left(\cosh \sqrt{2 \cdot 5^{5/4} \delta \gamma} t - 1 \right) \simeq \frac{5}{4} \gamma_c \left(\frac{N}{N_c} - 1 \right) t^2. \quad (33)$$

In contrast, the final stage of the collapse is dominated by the last term in Eq. (32) if $\delta \gamma \ll 1$, so that we obtain

$$x(t) \simeq \frac{3 \cdot 5^{-5/4}}{(t_{\text{collapse}} - t)^2}, \quad (34)$$

where the constant of integration t_{collapse} may be interpreted as the time scale for BEC to collapse. Because t_{collapse} is dominated by the slow initial stage of the collapse, its evaluation requires the inclusion of the first and third terms of Eq. (32), obtaining

$$\begin{aligned} t_{\text{collapse}} &= \int_0^\infty \frac{dx}{\sqrt{\frac{20}{3} \cdot 5^{1/4} x^3 + 5 \delta \gamma x}} \\ &\simeq \frac{(3/10)^{1/4}}{4\sqrt{\pi}} \Gamma\left(\frac{1}{4}\right)^2 \left(\frac{N}{N_c} - 1\right)^{-1/4} \\ &\simeq 1.37 \left(\frac{N}{N_c} - 1\right)^{-1/4}. \end{aligned} \quad (35)$$

It is interesting to note that this collapse time obeys the same power with respect to $|1 - N/N_c|$ as that of ω_M^{-1} for N just below N_c (see Eq. (27)).

To check the validity of these analytic results, we numerically integrate the time-dependent GP equation using the finite-difference method with the Crank-Nicholson scheme [8]. Figure 3 shows the time evolution of the peak height of the wave function $|\psi(r=0, t)|$, where we prepare an initial metastable state for $|\gamma|/\gamma_c > 1 - 10^{-7}$, suddenly increase $|\gamma|$ to $|\gamma|/\gamma_c = 1 + 10^{-2}$ at $t = 0$, and then let the state evolve in time according to the GP equation (6) without atomic loss or to the GP equation (38) with the atomic loss. The dashed curve is obtained by solving Eq. (6), and the solid curve is obtained by solving Eq.(38) which includes the atomic-loss processes due to two-body dipolar loss and three-body recombination loss. In the initial stage of the collapse, the peak density grows slowly, and at $t \simeq 2.52$ the rapid implosion breaks out, where its blowup is shown in the inset. When the atomic loss is not included, the peak density increases to infinity (dashed curve).

Figure 4 shows the profiles of the wave functions $|\psi(r, t)|$ obtained by numerically solving the GP equation without loss processes (6) (solid curves) and the corresponding Gaussian functions that has the same width $\langle \hat{r} \rangle$ (dashed curves). Even at $t = 0$, the wave function deviates from the Gaussian function, particularly near the center of BEC. This deviation is the origin of the 17 % discrepancy in N_c between the numerically exact value and that obtained using the Gaussian trial wave function. During the initial stage of a gradual increase in the peak density, the deviation between the numerically obtained

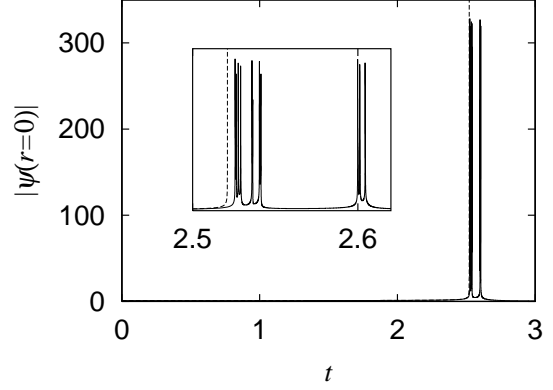


FIG. 3. Time evolution of the peak value $|\psi(r=0, t)|$ of the wave function. The solid curve shows a case with two-body dipolar loss and with three-body recombination loss (Eq. (38)), and the dashed curve without these losses (Eq. (6)). We first prepare BEC in a metastable state slightly below the critical point, and at $t = 0$, increase N so that $N/N_c - 1 = 10^{-2}$. The inset shows a blow-up view of the intermittent implosion.

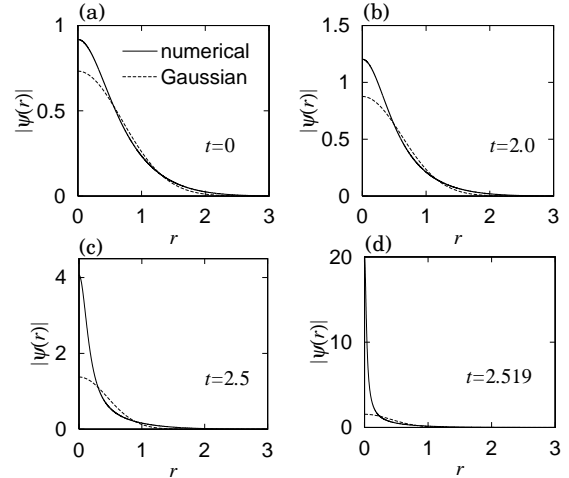


FIG. 4. The solid curves show the profiles of the wave functions $|\psi(r, t)|$ at $t = 0, 2, 2.5$, and 2.519 , obtained by numerically solving the Gross-Pitaevskii equation (6) for the same conditions as in Fig. 3. The dashed curves show Gaussian functions having the same $\langle \hat{r} \rangle$ as each wave function (for the definition of $\langle \hat{r} \rangle$, see the text).

and Gaussian wave function does not grow so much (see Fig. 4 (b)). At and after the outbreak of the implosion (Figs. 4 (c) and (d)), however, the deviation becomes significant, and the Gaussian approximation apparently breaks down, as the implosion occurs in the small region at the center. The implosion occurs suddenly, so we may define $t_{\text{implosion}}$ as the time at which the rapid implosion occurs.

Until the rapid implosion takes place, the Gaussian

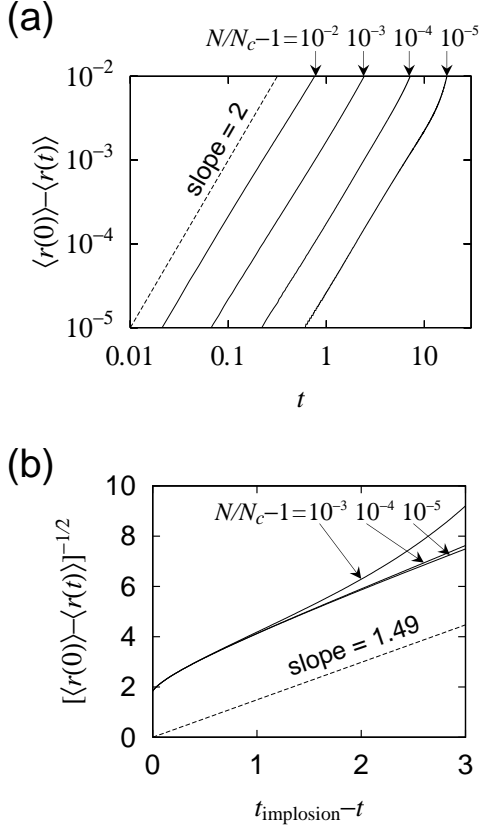


FIG. 5. (a) The time development of $\langle \hat{r}(0) \rangle - \langle \hat{r}(t) \rangle$ obtained by numerically solving the Gross-Pitaevskii equation (6) for $N/N_c - 1 = 10^{-2}, 10^{-3}, 10^{-4}$, and 10^{-5} . BEC is initially prepared in a metastable state for N just below N_c , and N is suddenly increased above N_c . (b) The time development of $[\langle \hat{r}(0) \rangle - \langle \hat{r}(t) \rangle]^{-1/2}$ obtained by numerically solving the Gross-Pitaevskii equation (6) for $N/N_c - 1 = 10^{-3}, 10^{-4}$, and 10^{-5} , as functions of $t_{\text{implosion}} - t$, where $t_{\text{implosion}}$ is the time at which the rapid implosion occurs. The dashed line shows the slope of $(3 \cdot 5^{-5/4} 2/\sqrt{\pi})^{-1/2} \simeq 1.49$ for reference.

trial wave function fairly well describes the collapsing dynamics. Figure 5 shows the time evolution of $\langle \hat{r}(0) \rangle - \langle \hat{r}(t) \rangle$ at the initial and final stages of the collapse, which is obtained by numerically solving the lossless GP equation (6). The expectation value $\langle \hat{r}(t) \rangle$ is defined as

$$\langle \hat{r}(t) \rangle \equiv \int r |\psi_{\text{var}}(\mathbf{r}, t)|^2 d\mathbf{r} = \frac{2}{\sqrt{\pi}} r(t), \quad (36)$$

where $\psi_{\text{var}}(\mathbf{r}, t)$ denotes the Gaussian variational wave function (9) and $r(t)$ is the variational parameter, and hence $\langle \hat{r}(0) \rangle - \langle \hat{r}(t) \rangle$ corresponds to $2x(t)/\sqrt{\pi}$, where $x(t) \equiv r_c - r(t)$. The initial changes in the width of the wave functions, shown in Fig. 5 (a), fit the square of t well, and the prefactors are proportional to $N/N_c - 1$, in agreement with Eq. (33). Figure 5 (b) shows $[\langle \hat{r}(0) \rangle - \langle \hat{r}(t) \rangle]^{-1/2}$ at the final stage of the collapse. The curves become linear as they approach $t = t_{\text{implosion}}$, with the slope being close to $(3 \cdot 5^{-5/4} \cdot 2/\sqrt{\pi})^{-1/2} \simeq 1.49$, in

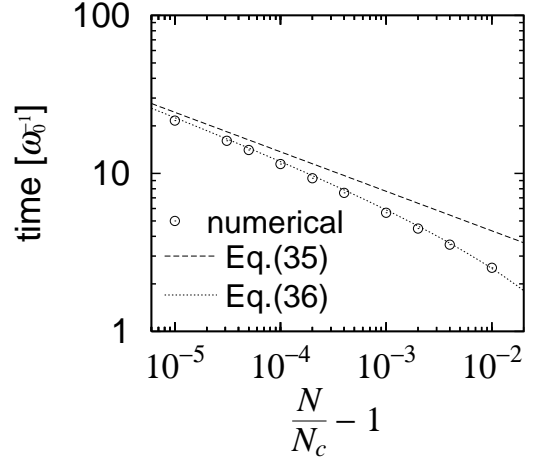


FIG. 6. The time it takes BEC to collapse as a function of $N/N_c - 1$ for N above N_c . The open circles represent times at which the rapid implosions occur, all of which are obtained by numerically solving the Gross-Pitaevskii equation (6). The dashed line shows Eq. (35), and the dotted curve shows Eq. (37) with $\Delta t = 1.83$.

agreement with the inverse-square behavior in Eq. (34). The curves end at a finite value $[\langle \hat{r}(0) \rangle - \langle \hat{r}(t) \rangle]^{-1/2} \simeq 2$ at $t = t_{\text{implosion}}$, since the rapid implosion occurs at this time.

The time $t_{\text{implosion}}$ is determined by numerically solving the GP equation (6), while t_{collapse} , given in Eq. (35), is analytically derived by using the Gaussian approximation and the small-deviation approximation (32). Although these approximations break down just before the implosion, t_{collapse} should still give the time scale of the collapsing dynamics, for the time it takes BEC to collapse is dominated by the slow initial stage, where the approximations are valid. Quantitatively, however, t_{collapse} overestimates the correct implosion time $t_{\text{implosion}}$ because Eq. (32) neglects higher-order terms that accelerate the implosion at the final stage of the collapse. Figure 6 shows t_{collapse} (dashed line) and numerically obtained $t_{\text{implosion}}$ (open circles). Since the difference between $t_{\text{implosion}}$ and t_{collapse} comes from the final stage of the collapse and we consider the case in which the initial numbers of atoms are almost the same, their relation may be given by

$$t_{\text{implosion}} = t_{\text{collapse}} - \Delta t, \quad (37)$$

where Δt is a constant that should be determined from a numerical analysis. The dotted curve in Fig. 6 represents Eq. (37) with $\Delta t = 1.83$, which is in excellent agreement with the numerically obtained exact $t_{\text{implosion}}$. For small $N/N_c - 1$, $t_{\text{implosion}}$ asymptotically approaches t_{collapse} (dashed line), which is governed by the power law $\propto (N/N_c - 1)^{-1/4}$.

V. INTERMITTENT IMPLOSION AND EXPLOSION

If the atomic loss is not included in the GP equation, the peak density grows to infinity, as shown in Fig. 3 (dashed curve). In actual experiments, when the density becomes very high, the atomic loss due to inelastic collisions becomes important. We, therefore, employ the GP equation with loss processes [21] as

$$i\frac{\partial}{\partial t}\psi = -\frac{1}{2}\nabla^2\psi + \frac{r^2}{2}\psi + g|\psi|^2\psi - \frac{i}{2}\left(\frac{L_2}{2}|\psi|^2 + \frac{L_3}{6}|\psi|^4\right)\psi, \quad (38)$$

where L_2 and L_3 denote the two-body dipolar and three-body recombination loss-rate coefficients, respectively. The two-body (three-body) loss-rate coefficient must be divided by two (six) because of Bose statistics [32]. In Eq. (38), L_2 and L_3 are made dimensionless by multiplying $N/(\omega_0 d_0^3)$ and $N^2/(\omega_0 d_0^6)$, respectively. The atoms and molecules produced by inelastic collisions are assumed to escape from the trap without affecting the condensate.

The solid curve in Fig. 3 shows the time evolution of the peak height of the wave function $|\psi(r=0, t)|$ following Eq. (38), where we assume a ^7Li condensate with $N = 1260$, $\omega_0 = 2\pi \times 144.5$ Hz [24], $L_2 = 1.05 \times 10^{-14}$ cm³/s [33], and $L_3 = 2.6 \times 10^{-28}$ cm⁶/s [34]. The initial condition is the same as the lossless case (dashed curve). During the gradual increase in the peak density, a few atoms are lost, which slightly delays the time of implosion. When the implosion begins, the role of the atomic loss becomes significant. The implosion stops at a certain density, showing pulse-like behavior (see the inset of Fig. 3), and occurs several times intermittently in rapid sequence [27]. This behavior may be qualitatively explained as follows. When the rapid implosion occurs and the peak density satisfies $g|\psi|^2 \sim L_3|\psi|^4/12$, i.e., $|\psi|^2 \sim 12g/L_3$, the collisional loss rate begins to surmount the accumulation rate of atoms at the center. When the atoms at the peak are suddenly removed due to atomic loss, the attractive force within a small spatial region is weakened, and the atoms begin to explode rather than implode due to the zero-point kinetic pressure. When the inward flow outside the region of implosion is sufficient to replenish the peak density, the subsequent implosion occurs. The intermittent implosions thus occur as the result of a competition between the loss of atoms and their accumulation due to the attractive interaction; therefore, these implosions should be distinguished from other oscillatory behaviors due to various mechanisms such as collapse-and-growth cycles [22,23,21] and the small collapses described in Ref. [21]. In the case of ^7Li , the peak density is estimated to be $|\psi|^2 \sim 12g/L_3 \simeq 400^2$, which qualitatively agrees with the solid curve in Fig. 3. We should note

here that the peak density $|\psi|^2 \sim 48\pi\hbar a/(mL_3)$, where the dimension is restored, is independent of the number of atoms N and the trap frequency ω_0 , indicating that the implosions are a local phenomenon depending only on the nature of the atoms themselves.

The explosion following an implosion of atoms is predicted in Refs. [21,27] and has been experimentally observed as a broadly scattered “hot” atom cloud of about 100 nK [5]. From the above discussion, the energy scale of the explosion might be estimated as $g|\psi|^2 \sim 12g^2/L_3$. This energy is, however, the highest one that only a small number of atoms at the center of BEC may acquire. In fact, the atoms scattered by the explosion have a broad momentum distribution. Figure 7 (a) shows a normalized energy distribution of atoms scattered by the explosion, where the parameters of ^7Li are used; the lower panel of Fig. 7 (a) shows the same distribution with L_3 is multiplied by 100. These energy distributions are obtained from the wave functions at $t = t_{\text{implosion}} + \pi/2$, at which the ejected part of BEC spreads maximally and are therefore easy to be discerned from the remnant part of BEC that remains at the center. The energy per atom at position \mathbf{r} is given by

$$\psi^*(\mathbf{r})\left(-\frac{1}{2}\nabla^2 + \frac{r^2}{2}\right)\psi(\mathbf{r})/|\psi(\mathbf{r})|^2, \quad (39)$$

where the interaction energy is omitted since the density of the widespread atoms are low enough. In obtaining the energy distributions and the mean energies, the remnant part of the condensate at the center is excluded. While the energy scale is different, the two distributions in Fig. 7 (a) have similar shapes. The number of atoms scattered by the explosion is 20 ~ 40 % of the total number of atoms. The dependence of this fraction on the parameters g and L_3 is complicated, since it depends on the number of times and the detailed structure of the intermittent implosions that are governed by highly nonlinear dynamics.

Figure 7 (b) shows the mean energies of the atoms scattered by the explosion as a function of g^2/L_3 . The open circles are obtained using the value of g of ^7Li with $\omega_0 = 2\pi \times 144.5$ Hz and the three-body recombination rates L_3 , $10L_3$, and $100L_3$. In order to see the dependence on g , the value of g is halved in the solid circles. The open and solid circles have almost the same dependence on g^2/L_3 , suggesting that the explosion energy is determined by the ratio g^2/L_3 , and not by g and L_3 separately. The mean energy is roughly given by $\sim 0.1g^2/L_3$, or restoring the dimension by

$$\sim 0.1 \times 16\pi^2 \frac{\hbar^3 a^2}{m^2 L_3}. \quad (40)$$

We note that this energy is independent of the number of atoms N and the trap frequency ω_0 , as with the peak density discussed above. These results indicate that the

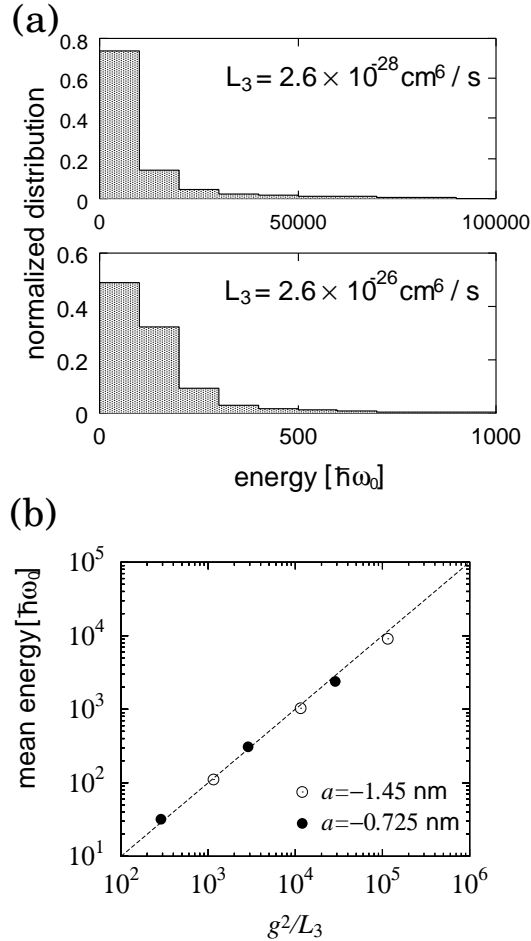


FIG. 7. (a) Normalized distributions of the energy of an atom scattered by the explosion. The same parameters and the initial conditions as those in the solid curve in Fig. 3 are used in the upper distribution, and the three-body recombination rate is multiplied by 100 in the lower one. (b) The mean energies of an scattered atom. The rightmost open circle is obtained using the parameters of ^7Li , and the other open circles are obtained by increasing the three-body recombination rate by 10 and 100. In the solid circles, the s-wave scattering length is halved.

global nature of the system is unimportant with regard to implosion and explosion, and that only the local nature of the atoms determines their behavior. Using Eq. (40), the mean kinetic energy of the atoms scattered by the explosion in the experiment at Rice [24] is estimated to be $\simeq 80\mu\text{K}$. In the experiment at JILA [5], on the other hand, the three-body recombination rate of ^{85}Rb is uncertain in the vicinity of the Feshbach resonance, where it significantly depends on the applied magnetic field [35]. The experiment of collapse is carried out by applying magnetic field of about 170 G at which sign of the interaction changes. Because of uncertainty in the three-body recombination rate, we estimate it from the experimen-

tal result of the explosion energy $\simeq 100\text{ nK}$ based on Eq. (40). Assuming $a = -1\text{ nm}$, we obtain $L_3 \simeq 6 \times 10^{-28}\text{ cm}^6/\text{s}$, which is consistent with the value of L_3 around 170 G [35]. The above-described method thus provides an independent way to determine the three-body recombination rate in addition to the current methods [36,37,35].

VI. CONCLUSIONS

We have analytically and numerically studied the dynamics of BEC with attractive interactions below and above the critical number of atoms N_c . We have shown that our analytic approach successfully describes the collective oscillations below N_c as well as the collapsing dynamics of BEC above N_c until the rapid implosion takes place. We have found that the time scales of the dynamics follow the same power law on either side of the critical point. Just below N_c , the collective frequency of the monopole mode is proportional to $(1 - N/N_c)^{1/4}$, and just above N_c , the time it takes BEC to collapse is proportional to $(N/N_c - 1)^{-1/4}$.

When the atomic loss due to inelastic collisions is taken into account, the implosion occurs not only once but several times intermittently, and the implosion is then converted to an explosion. We have found that the mean energy of an atom scattered by the explosion is given by Eq. (40), which is independent of the number of atoms and the trap frequency.

ACKNOWLEDGMENTS

This work was supported by a Grant-in-Aid for Scientific Research (Grant No. 11216204) by the Ministry of Education, Science, Sports, and Culture of Japan, and by the Toray Science Foundation.

-
- [1] M. H. Anderson, J. R. Ensher, M. R. Matthews, C. E. Wieman, and E. A. Cornell, *Science* **269**, 198 (1995).
 - [2] K. B. Davis, M. -O. Mewes, M. R. Andrews, N. J. van Druten, D. S. Durfee, D. M. Kurn, and W. Ketterle, *Phys. Rev. Lett.* **75**, 3969 (1995).
 - [3] D. G. Fried, T. C. Killian, L. Willmann, D. Landhuis, S. C. Moss, D. Kleppner, and T. J. Greytak, *Phys. Rev. Lett.* **81**, 3811 (1998).
 - [4] C. C. Bradley, C. A. Sackett, J. J. Tollett, and R. G. Hulet, *Phys. Rev. Lett.* **75**, 1687 (1995); **79**, 1170(E) (1997); C. C. Bradley, C. A. Sackett, and R. G. Hulet, *ibid.* **78**, 895 (1997).

- [5] S. L. Cornish, N. R. Claussen, J. L. Roberts, E. A. Cornell, and C. E. Wieman, Phys. Rev. Lett. **85**, 1795 (2000).
- [6] E. Tiesinga, A. Moerdijk, B. J. Verhaar, and H. T. C. Stoof, Phys. Rev. A **46**, R1167 (1992); E. Tiesinga, B. J. Verhaar, and H. T. C. Stoof, *ibid.* **47**, 4114 (1993).
- [7] S. Inouye, M. R. Andrews, J. Stenger, H. -J. Miesner, D. M. Stamper-Kurn, and W. Ketterle, Nature **392**, 151 (1998).
- [8] P. A. Ruprecht, M. J. Holland, K. Burnett, and M. Edwards, Phys. Rev. A **51**, 4704 (1995).
- [9] G. Baym and C. J. Pethick, Phys. Rev. Lett. **76**, 6 (1996).
- [10] A. L. Fetter, cond-mat/9510037.
- [11] F. Dalfovo and S. Stringari, Phys. Rev. A **53**, 2477 (1996).
- [12] R. J. Dodd, M. Edwards, C. J. Williams, C. W. Clark, M. J. Holland, P. A. Ruprecht, and K. Burnett, Phys. Rev. A **54**, 661 (1996).
- [13] M. Houbiers and H. T. C. Stoof, Phys. Rev. A **54**, 5055 (1996).
- [14] H. T. C. Stoof, J. Stat. Phys. **87**, 1353 (1997).
- [15] M. Ueda and A. J. Leggett, Phys. Rev. Lett. **80**, 1576 (1998).
- [16] Y. E. Kim and A. L. Zubarev, Phys. Lett. A **246**, 389 (1998).
- [17] M. Wadati and T. Tsurumi, Phys. Lett. A **247**, 287 (1998).
- [18] Yu. Kagan, G. V. Shlyapnikov, and J. T. M. Walraven, Phys. Rev. Lett. **76**, 2670 (1996).
- [19] E. V. Shuryak, Phys. Rev. A **54**, 3151 (1996).
- [20] C. Huepe, S. Métens, G. Dewel, P. Borckmans, and M. E. Brachet, Phys. Rev. Lett. **82**, 1616 (1999).
- [21] Yu. Kagan, A. E. Muryshev, and G. V. Shlyapnikov, Phys. Rev. Lett. **81**, 933 (1998).
- [22] C. A. Sackett, C. C. Bradley, M. Welling, and R. G. Hulet, Appl. Phys. B **65**, 433 (1997).
- [23] C. A. Sackett, H. T. C. Stoof, and R. G. Hulet, Phys. Rev. Lett. **80**, 2031 (1998).
- [24] C. A. Sackett, J. M. Gerton, M. Welling, and R. G. Hulet, Phys. Rev. Lett. **82**, 876 (1999); J. M. Gerton, D. Strekalov, I. Prodan, and R. G. Hulet, unpublished.
- [25] M. Ueda and K. Huang, Phys. Rev. A **60**, 3317 (1999).
- [26] A. Eleftheriou and K. Huang, Phys. Rev. A **61**, 043601 (2000).
- [27] H. Saito and M. Ueda, cond-mat/0002393.
- [28] E. P. Gross, Nuovo Cimento **20**, 454 (1961); J. Math. Phys. **4**, 195 (1963); L. P. Pitaevskii, Zh. Eksp. Teor. Fiz. **40**, 646 (1961) [Sov. Phys. JETP **13**, 451 (1961)].
- [29] V. M. Pérez-García, H. Michinel, J. I. Cirac, M. Lewenstein, and P. Zoller, Phys. Rev. Lett. **77**, 5320 (1996); Phys. Rev. A **56**, 1424 (1997).
- [30] S. Stringari, Phys. Rev. Lett. **77**, 2360 (1996).
- [31] M. Edwards, R. J. Dodd, C. W. Clark, and K. Burnett, J. Res. Natl. Inst. Stand. Technol. **101**, 553 (1996).
- [32] Yu. Kagan *et al.*, JETP Lett. **42**, 209 (1985); H. T. C. Stoof, A. M. L. Janssen, J. M. V. A. Koelman, and B. J. Verhaar, Phys. Rev. A **39**, 3157 (1989).
- [33] J. M. Gerton, C. A. Sackett, B. J. Frew, and R. G. Hulet, Phys. Rev. A **59**, 1514 (1999).
- [34] A. J. Moerdijk, H. M. J. M. Boesten, and B. J. Verhaar, Phys. Rev. A **53**, 916 (1996).
- [35] J. L. Roberts, N. R. Claussen, S. L. Cornish, and C. E. Wieman, Phys. Rev. Lett. **85**, 728 (2000).
- [36] E. A. Burt, R. W. Ghrist, C. J. Myatt, M. J. Holland, E. A. Cornell, and C. E. Wieman, Phys. Rev. Lett. **79**, 337 (1997).
- [37] D. M. Stamper-Kurn, M. R. Andrews, A. P. Chikkatur, S. Inouye, H. -J. Miesner, J. Stenger, and W. Ketterle, Phys. Rev. Lett. **80**, 2027 (1998).